GRAFT VERSUS HOST DISEASE

ST2 blockade reduces sST2-producing T cells while maintaining protective mST2-expressing T cells during graft-versus-host disease

Jilu Zhang,[1,2,3,4] Abdulraouf M. Ramadan,[1,2,3,4] Brad Griesenauer,[1,2,3,4] Wei Li,[1,2,3,4] Matthew J. Turner,[2,5,6] Chen Liu,[7] Reuben Kapur,[2] Helmut Hanenberg,[1,2,8] Bruce R. Blazar,[9] Isao Tawara,[10] Sophie Paczesny[1,2,3,4]*

Graft-versus-host disease (GVHD) remains a devastating complication after allogeneic hematopoietic cell transplantation (HCT). We previously identified high plasma soluble suppression of tumorigenicity 2 (sST2) as a biomarker of the development of GVHD and death. sST2 sequesters interleukin-33 (IL-33), limiting its availability to T cells expressing membrane-bound ST2 (mST2) [T helper 2 (T_H2) cells and $ST2^+FoxP3^+$ regulatory T cells]. We report that blockade of sST2 in the peritransplant period with a neutralizing monoclonal antibody (anti-ST2 mAb) reduced GVHD severity and mortality. We identified intestinal stromal cells and T cells as major sources of sST2 during GVHD. ST2 blockade decreased systemic interferon-γ, IL-17, and IL-23 but increased IL-10 and IL-33 plasma levels. ST2 blockade also reduced sST2 production by IL-17–producing T cells while maintaining protective mST2-expressing T cells, increasing the frequency of intestinal myeloid–derived suppressor cells, and decreasing the frequency of intestinal CD103 dendritic cells. Finally, ST2 blockade preserved graft-versus-leukemia activity in a model of green fluorescent protein (GFP)–positive MLL-AF9 acute myeloid leukemia. Our findings suggest that ST2 is a therapeutic target for severe GVHD and that the ST2/IL-33 pathway could be investigated in other T cell–mediated immune disorders with loss of tolerance.

INTRODUCTION

Allogeneic hematopoietic cell transplantation (allo-HCT) is an essential therapeutic modality for patients with hematological malignancies and other blood disorders. The most common indications for allo-HCT are acute myeloid leukemias and myelodysplastic syndromes. In these patients, the beneficial effects of allo-HCT are based on immune-mediated elimination of leukemic cells through the graft-versus-leukemia (GVL) activity of donor T cells, the most validated immunotherapy to date (*1*–*3*). Unfortunately, donor T cells also mediate damage to normal host tissues, potentially leading to graft-versus-host disease (GVHD) (*4*, *5*). GVHD remains the major complication of allo-HCT and is associated with high mortality, morbidity, and health care costs. Current strategies to control GVHD rely on global immunosuppression, for which little progress has been made since the introduction of calcineurin inhibitor–based regimens in the mid-1980s. Despite standard prophylaxis with these regimens, acute and chronic GVHD still develop in about 40 to 60% of allo-HCT recipients (*6*–*8*). In addition, nonselective immunosuppression approaches can decrease GVL activity, increasing the risk of leukemia relapse (*3*, *9*). Therefore, new approaches are needed to prevent GVHD without diminishing GVL efficacy.

We recently reported that high plasma levels of suppression of tumorigenicity 2 (ST2) at day 14 after HCT is a prognostic biomarker for the development of GVHD and death (*10*). ST2, also known as interleukin-33 receptor (IL-33R), is the newest member of the IL-1 receptor family, and its only known ligand is IL-33 (*11*). Due to alternative splicing, ST2 has two main isoforms: a membrane-bound form (mST2) and a soluble form (sST2) (*12*). mST2 consists of three extracellular immunoglobulin domains and an intracellular Toll-like receptor domain, which associates with the IL-1R accessory protein to induce MyD88 (myeloid differentiation primary response gene 88)–dependent signaling. ST2 is expressed on various innate and adaptive immune cell types and drives the production of type 2 cytokines, which are responsible for protective type 2 inflammatory responses in infection and tissue repair as well as detrimental allergic responses (*11*, *13*–*17*). sST2 lacks the transmembrane and intracellular Toll-like receptor domains and functions only as a decoy receptor to sequester free IL-33 (*17*–*19*).

As a reflection of the role of the IL-33/ST2 signaling pathway in allogeneic reactions, sST2 concentrations are increased in acute cardiac allograft rejection (*20*), and treatment with IL-33 prolongs allograft survival through the expansion of regulatory T cells (T_{regs}) and myeloid-derived suppressor cells (MDSCs) (*21*, *22*). sST2 levels are also increased in patients with active inflammatory bowel disease (*23*, *24*), a condition similar to gastrointestinal (GI) GVHD. sST2 increase has been suggested to represent a mechanism by which intestinal inflammatory pathogenic responses are perpetuated by limiting IL-33–driven $ST2^+$ T_{reg} accumulation and function in the intestine (*25*). Although both proinflammatory and anti-inflammatory roles have been reported for IL-33 (*11*), in the disease models mentioned above, IL-33 had a clear anti-inflammatory role particularly by signaling through the mST2 on T_{regs} that results in an up to 20% greater steady-state level of total T_{regs} in the gut (*25*). Here, due to the

[1]Department of Pediatrics, Indiana University School of Medicine, Indianapolis, IN 46202, USA. [2]Herman B. Wells Center for Pediatric Research, Indiana University School of Medicine, Indianapolis, IN 46202, USA. [3]Department of Microbiology and Immunology, Indiana University School of Medicine, Indianapolis, IN 46202, USA. [4]Melvin and Bren Simon Cancer Center, Indiana University School of Medicine, Indianapolis, IN 46202, USA. [5]Department of Dermatology, Indiana University School of Medicine, Indianapolis, IN 46202, USA. [6]Richard L. Roudebush Veterans Affairs Medical Center, Indianapolis, IN 46202, USA. [7]Department of Pathology and Immunology, University of Florida College of Medicine, Gainesville, FL 32610, USA. [8]Department of Medical and Molecular Genetics, Indiana University School of Medicine, Indianapolis, IN 46202, USA. [9]Department of Pediatrics, University of Minnesota, Minneapolis, MN 55454, USA. [10]Department of Hematology/Oncology, Mie University Hospital, Mie 514-8507, Japan.
*Corresponding author. E-mail: sophpacz@iu.edu

similarities with the colitis models, namely, the elevated plasma level of the IL-33 decoy receptor sST2, and because the GI tract is the main GVHD target organ, we hypothesized that sST2 has a proinflammatory role due to its decoy activity and that IL-33 plays an anti-inflammatory role through an increase in $ST2^+$ T_{regs} and MDSCs in the GI tract.

Whether sST2 is a key player in the development of GVHD or only a circulating molecule indicating increased GVHD risk has remained unclear. Furthermore, it was unclear whether sST2 could be drug-targetable and therefore used to alleviate GVHD. Here, we investigated the effects of sST2 blockade using anti-ST2 monoclonal antibody (mAb) on GVHD severity and mortality in a clinically relevant model of HCT and the GVL effects against retrovirally transduced green fluorescent protein (GFP)–positive MLL-AF9 acute myeloid leukemia. We also tested the hypotheses that, during GVHD, the ratio of sST2 to mST2 is increased and that the major source of sST2 is the GI tract. Therefore, blocking the excess sST2 with anti-ST2 mAb would inhibit its decoy activity and release free IL-33 to bind the mST2 receptor to mST2-expressing T cells [T helper 2 (T_H2) cells and $ST2^+FoxP3^+$ T_{regs}] that we found to be protective in our GVHD model. Because no anti-ST2 mAb specific to the soluble form was available to us, we used the full-length anti-ST2 mAb available from Centocor (CNT03914) (*26*) and tested several doses and schedules to identify a treatment course that would inhibit sST2 without inhibiting mST2. Our results indicate that anti-ST2 mAb represents a therapeutic modality for the safe and efficient targeting of sST2 to control severe GVHD. Our findings also suggest that sST2 secreted by intestinal stromal/endothelial cells and intestinal alloreactive T cells limits the local and systemic expansion and function of mST2-expressing cells, particularly T_H2 cells and $ST2^+FoxP3^+$ T_{regs}, by antagonizing IL-33 activity and reducing its bioavailability. Because aberrant ST2/IL-33 signaling has been linked to many human diseases, the results of this study may have broad implications in other T cell–mediated immune disorders.

RESULTS

Similar to GVHD patients, experimental models of allo-HCT show increased plasma concentrations of sST2 before GVHD onset

To determine whether sST2 might contribute to GVHD similarly to observations in patients, we first assessed the kinetics of plasma sST2 in a minor histocompatibility antigen (miHA)–mismatched model of allo-HCT and a human-to-mouse xenogeneic model. Donor T cells derived from C57BL/6 (B6) mice or human T cells were transplanted into irradiated miHA-mismatched C3H.SW or xenogeneic NOD-*scid*IL2Rγ^{null} (NSG) mice, respectively, to induce GVHD. Mice receiving syngeneic T cells or irradiation only were used as controls. As expected, all allogeneic/xenogeneic recipient mice receiving donor T cells developed severe GVHD, with about 80% dying of GVHD. By contrast, mice receiving syngeneic cells did not develop any clinical signs of GVHD. Enzyme-linked immunosorbent assay (ELISA) analysis showed that the plasma sST2 concentration was significantly increased in mice receiving allogeneic/xenogeneic HCT, but not in syngeneic or irradiation-only controls, by day 10 and day 21 after transplantation, mimicking the kinetics observed in patients (*10*) (Fig. 1, A and C).

sST2 can be blocked by a neutralizing anti-ST2 mAb, leading to a decrease in proinflammatory and an increase in anti-inflammatory cytokine plasma levels and decreased acute GVHD severity and mortality

Given the high levels of circulating sST2, we hypothesized that sST2 blockade can ameliorate GVHD severity by blocking its decoy receptor activity and thus releasing free IL-33 that will be used by mST2-expressing T cells. We used a mAb targeting murine ST2 (anti-ST2 mAb) (CNT03914) or an appropriate control isotype antibody [immunoglobulin G (IgG)] (*26*). We used the miHA model B6→C3H.SW, as it is the most clinically relevant not only because about 80% of HCTs performed today in the United States are 8/8 major histocompatibility complex (MHC)–matched [the Center for International Blood and Marrow Transplant Research (CIBMTR) data as a personal communication] but also because GVHD is both CD8- and CD4-dependent (*5*). The anti-ST2 mAb and IgG control (both at 100 μg/dose) were administered to mice via intraperitoneal injection every other day from day −1 to day +9 after HCT. Anti-ST2 mAb blockade strongly attenuated GVHD and increased survival (fig. S1A and table S3). Histopathological scores in the small intestine, large intestine, and liver (primary GVHD target organs) were improved in anti-ST2 mAb–treated mice, suggesting that ST2 blockade alleviated GVHD severity in the main target organs (fig. S1B). We then evaluated a shorter schedule of anti-ST2 mAb treatment with only two doses administered on day −1 and day +1 of HCT. Transient blockade of ST2 in the peritransplant period was sufficient to provide long-lasting protection against GVHD (Fig. 1B). We next tested ST2 blockade in the human-to-mouse xenogeneic GVHD model, and the results showed alleviation of GVHD and improved survival (Fig. 1D). Systemic production of the inflammatory cytokines interferon-γ (IFN-γ), IL-17, and IL-23 was decreased, whereas the release of anti-inflammatory cytokines IL-10 and IL-33 was increased in the plasma (Fig. 1E).

The GI tract is the major sST2-producing organ during GVHD

To understand the basis for the effects of sST2 blockade, we determined the source of sST2 after allo-HCT. At day 10 after HCT, before the onset of GVHD, the quantitative mRNA expression of both sST2 and mST2 was analyzed in the spleen, small intestine, large intestine, skin, bone marrow (BM), lung, heart [as a representative organ for the endothelium and a known source of sST2 (*20*, *27*)], liver, and peripheral blood. The small and large intestines were by far the largest producers of sST2, even compared to the heart (Fig. 2A, left), and strikingly, they also showed the lowest levels of mST2 expression (Fig. 2A, middle). Therefore, the sST2/mST2 ratio was increased in the GI tract of mice that developed GVHD (Fig. 2A, right).

Intestinal stromal and endothelial cells a major source of sST2 that is neutralized by anti-ST2 mAb, and $ST2^{-/-}$-deficient recipients exhibit less severe GVHD

sST2 can be produced by a number of different cell types, and we found that sST2 is produced highly in the intestine. Therefore, we investigated the cellular source of sST2 in the intestine. Intestinal stromal cells that are $CD45^-EpCAM^-$ and endothelial cells that are $CD45^-EpCAM^-CD146^+$ were major producers of sST2 during GVHD, whereas epithelial cells that are $CD45^-EpCAM^+$ did not produce sST2 (Fig. 2B). In addition, myeloid cells [$CD45^+$TCRβ (T cell receptor β)$^-$] produced only a small amount of sST2. To confirm that the host-derived origin of sST2 production is necessary for GVHD development, we used

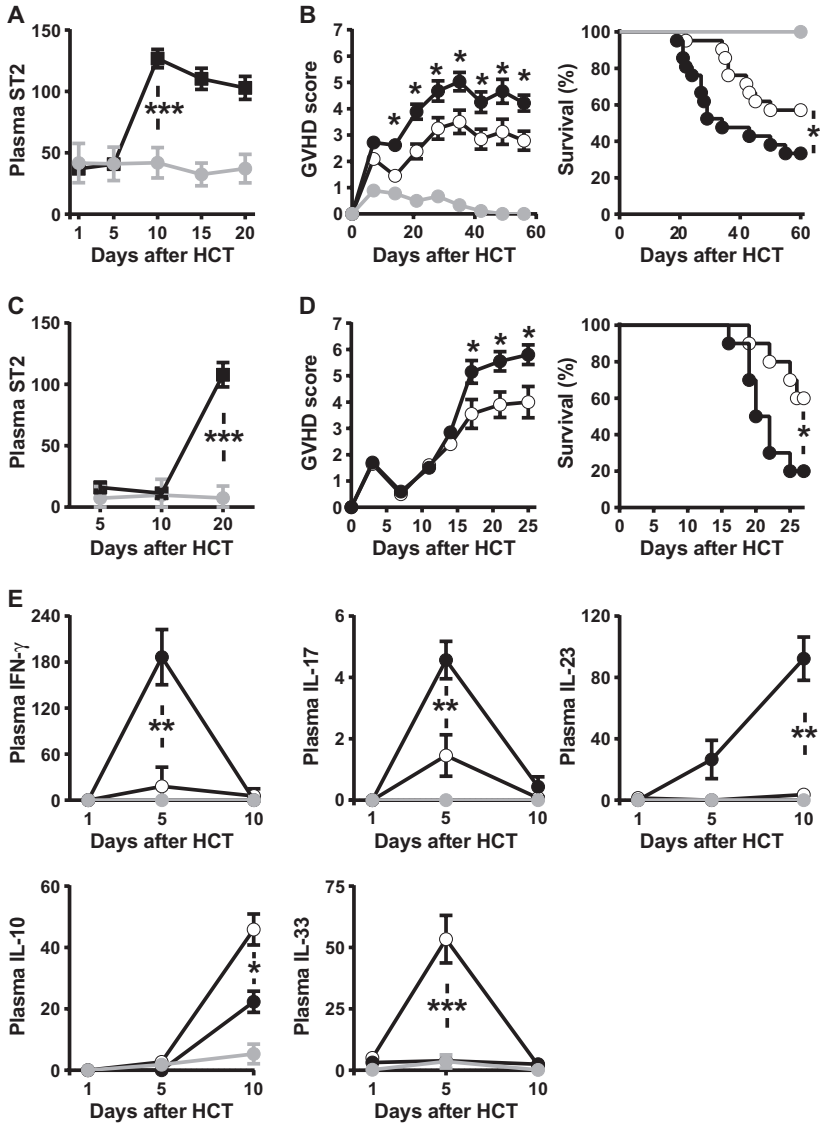

Fig. 1. ST2 blockade and GVHD. (**A**) Irradiated C3H.SW mice (1100 cGy) were transplanted with syngeneic (●) or allogeneic B6 (■) BM cells (5×10^6) and splenic purified T cells (2×10^6). sST2 concentrations in plasma collected at the indicated times after HCT from C3H.SW recipients (ng/ml) ($P = 0.0001$, *t* test; $n = 10$ to 12). The data are from four independent experiments. (**B**) Clinical scores of GVHD and survival curves for C3H.SW mice receiving syngeneic (●) or allogeneic B6 cells and treated with anti-mouse ST2 antibody (○) or IgG control antibody (●) at day −1 and day +1 after HCT. The data are from three independent experiments (*P* values for GVHD scores are given in table S1; $P = 0.0256$ for survival analysis, *t* test for GVHD score and log-rank test for survival analysis; $n = 15$ to 23 per group). (**C**) Irradiated NSG mice (350 cGy) received 2.5×10^6 T cells purified from peripheral blood mononuclear cells (PBMCs) of healthy donors (■). The control group was irradiated without receiving human T cells (●). Human soluble ST2 concentrations in plasma collected at the indicated times after HCT from NSG recipient mice with or without engrafted human T cells (pg/ml). The data are from three independent experiments ($P = 0.0028$, *t* test; $n = 7$ to 9 per group). (**D**) Clinical scores of GVHD and survival curves for NSG mice receiving human T cells and treated with anti-human and anti-mouse ST2 antibodies (○) or IgG control antibody (●) every other day from day −1 to day +5 (four doses) (*P* values for GVHD scores are given in table S1, $P = 0.0329$ for survival analysis; *t* test for GVHD score and log-rank test for survival analysis; $n = 10$ per group). (**E**) IFN-γ, IL-17, IL-23, IL-10, and IL-33 concentrations in plasma collected every 5 days after HCT from the B6→C3H.SW model (pg/ml). The data are from three independent experiments. Syngeneic group (●); allogeneic groups treated with anti-ST2 (○) or IgG control (●) (*P* values are given in table S1; *t* test; $n = 3$ to 9 per group).

B6 $ST2^{-/-}$ mice as recipients and showed that sST2 deficiency in recipients reduced the GVHD score and prolonged the survival of the C3H.SW→B6 model (fig. S2 and table S3). Furthermore, anti-ST2 mAb blockade decreased sST2 production by stromal cells compared to that in IgG control–treated animals (Fig. 2C). These data suggest that production of sST2 by host stromal cells plays an important role in GVHD and that anti-ST2 blockade can diminish this production.

Intestinal T cells are the other major cellular source of sST2 during GVHD, and T cell production of sST2 is decreased by ST2 blockade

Strikingly, while determining the source of intestinal sST2, we discovered that T cells, mostly $CD4^+$ T cells, produced sST2 at the transcript (Fig. 2D) and protein levels (Fig. 2E). Secretion of sST2 by T cells significantly increased during GVHD progression (Fig. 2D). We next hypothesized that anti-ST2 mAb treatment would reduce the production of sST2 by alloreactive T cells in targets organs. Indeed, intestinal sST2 production by T cells was decreased in anti-ST2 mAb–treated animals (Fig. 2E). To explore further which T cell subsets produce sST2 and express mST2 during in vitro differentiating conditions, we measured sST2 production and mST2 expression in the CD4 subsets T_H1, T_H2, and T_H17, as well as the CD8 subsets T cytotoxic 1 (T_c1), T_c2, and T_c17. T_H17 and T_c17 cells were found to be strong producers of sST2 (Fig. 2F, left) and to express only low levels of mST2 protein (fig. S3). Similar results were observed in human T cell subsets (Fig. 2F, right).

ST2 deficiency reduces the ratio of sST2-secreting T cells to mST2-expressing T cells

Whole transcriptome analysis of mesenteric lymph node (MLN) T cells comparing anti-ST2 mAb–treated mice versus IgG control–treated mice showed that anti-ST2 treatment modulated the gene expression of T_H cell cytokines (Fig. 3A). To further assess the effects of ST2 blockade on the T_H cell compartment, we examined the sST2-secreting/mST2-expressing T cell balance at the protein level by flow cytometry. ST2 blockade decreased the percentages of T_H1 cells and pathogenic T_H17 cells (Fig. 3, B and C). To verify the role of donor sST2 in GVHD, we next used $ST2^{-/-}$ donor T cells in recipients of allo-HCT. Given that $ST2^{-/-}$ donor T cells are incapable of producing sST2, they had a protective effect on GVHD severity and increased survival (Fig. 3D). Recipients of $ST2^{-/-}$ donor T cells showed lower frequencies of IFN-γ/Tbet–producing T cells (Fig. 3E) and IL-17/RORγt–producing T cells (Fig. 3F) and less proliferation of $IFN\text{-}\gamma^+IL\text{-}17^+$ pathogenic T_H17 cells, as measured by Ki67, at day 10 after transplantation in the GI tract (Fig. 3G).

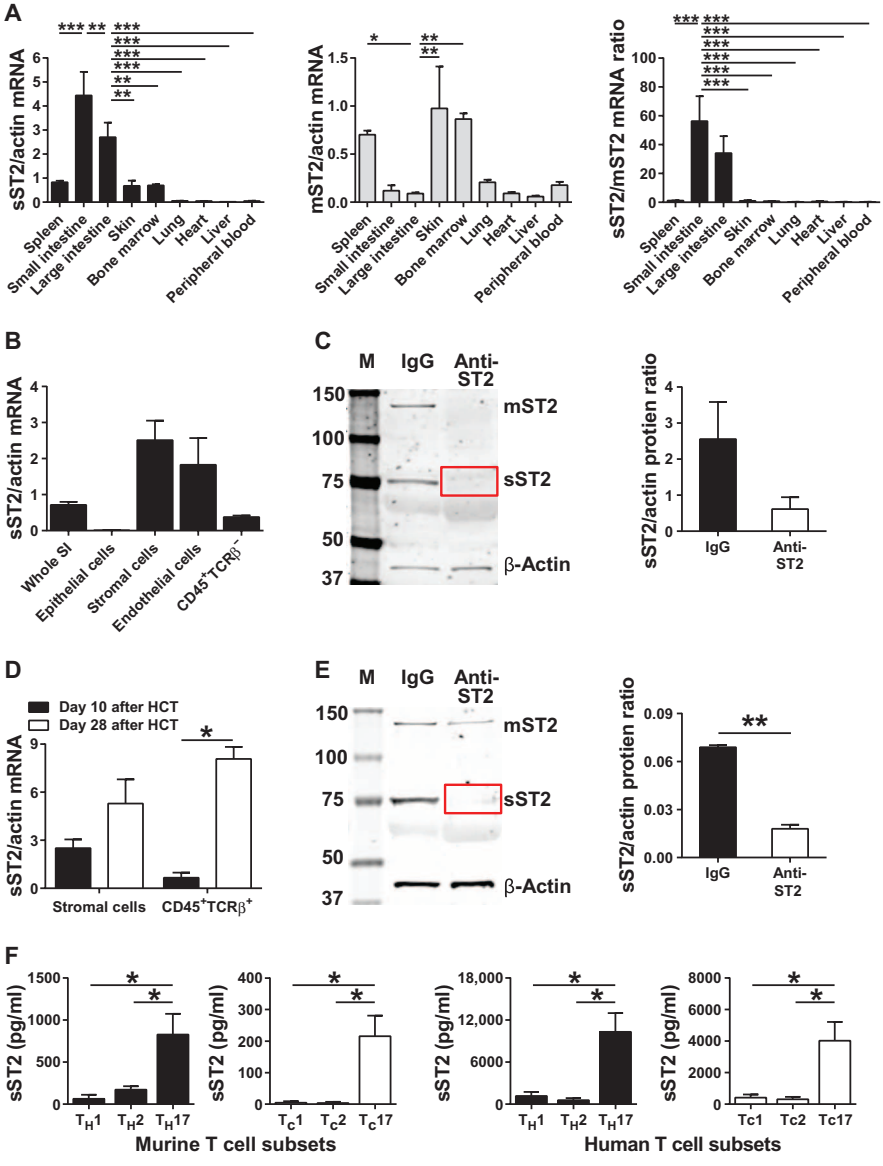

Fig. 2. sST2 and mST2 expression during GVHD. (**A**) In the B6→C3H.SW model, mRNA expression of sST2 and mST2 in different organs (spleen, small intestine, large intestine, skin, BM, lung, heart, liver, and peripheral blood) of C3H.SW recipient mice at day 10 after allo-HCT. The data are from four independent experiments [*P* values are given in table S2, one-way analysis of variance (ANOVA); *n* = 4]. (**B**) sST2/actin mRNA expression in intestine or intestinal cell subsets (epithelial, stromal, endothelial, or non–T hematopoietic cells) from C3H.SW recipient mice at day 10 after allo-HCT (*n* = 5). The data are from two independent experiments with two to three pooled mice. SI, small intestine. (**C**) Western blot analysis of sorted intestinal stromal cells from IgG control– or anti-ST2 mAb–treated C3H.SW recipient mice at day 10 after allo-HCT [M, marker (kD)] (left). The red box indicates the lack of sST2 protein present after anti-ST2 treatment. The bar graph shows the sST2/actin ratio in IgG control– or anti-ST2–treated mice (*n* = 6). The data are from two independent experiments with three pooled mice. (**D**) sST2/actin expression on sorted intestinal stromal and T cells from C3H.SW mice at day 10 and day 28 after allo-HCT. The data are from two independent experiments with two to three pooled mice (*P* = 0.0120, *t* test; *n* = 5). (**E**) Western blot analysis of sorted intestinal T cells from IgG control– or anti-ST2 mAb–treated C3H.SW recipients 10 days after allo-HCT [M, marker (kD)]. The red box indicates the lack of sST2 protein present after anti-ST2 treatment. The unmodified blots are shown in fig. S9. The bar graph shows the sST2/actin ratio in CD4 T cells from IgG–control or anti-ST2–treated mice. The data are from two independent experiments with three pooled mice (*P* = 0.0032, *t* test; *n* = 6). (**F**) sST2 secretion by both murine and human in vitro differentiated T cell subsets. The data are from three to four independent experiments (*P* values are given in table S2; *t* test; *n* = 3 to 4). The unmodified blots are shown in fig. S9.

At the same time, ST2 blockade increased the percentages of the T_H2 cytokine IL-4 and the T_H2 transcription factor GATA3 in T cells (Fig. 3H), as well as increased the frequency of FoxP3$^+$ T_{regs} (Fig. 3J). Transient ST2 blockade maintained mST2 expression on GATA3$^+$ T_H2 cells (Fig. 3H) and FoxP3$^+$ T_{regs} (Fig. 3J). IL-4/GATA3–producing T_H2 cells (Fig. 3I) as well as total FoxP3$^+$ T_{regs} and IL-10–producing T cells (Fig. 3K) were increased when ST2$^{-/-}$ donor T cells were used as the graft source, confirming the negative impact of wild-type donor T cells on GVHD through production of sST2. We next specifically investigated the impact of ST2$^+$FoxP3 T_{regs} in GVHD. For this, we used the B6→C3H.SW model with ST2$^{-/-}$ donor T_{regs} [ratio of T_{regs}/T_{conv} (conventional T cells) of 1:10] and demonstrated that recipients of wild-type donor T_{regs} had less severe GVHD and improved survival compared to recipients of ST2$^{-/-}$ T_{regs} (Fig. 3L). These results suggest, similarly to the observed colonic inflammation (*25*), that wild-type donor T_{regs} have a better suppressive capacity than ST2$^{-/-}$ T_{regs} and that mST2 expression on T_{regs} is important for GVHD protection.

ST2 deficiency induces expansion of tolerogenic MDSCs and inhibits immunogenic CD103 dendritic cells

Because IL-33 has been shown to induce expansion of MDSCs that have a potent T cell-suppressive function (*21*, *22*), we explored the effects of ST2 deficiency on intestinal antigen-presenting cell subsets. First, 99% of the antigen-presenting cell populations found in the intestine at day 10 after HCT are of donor origin (fig. S4, A and B). Second, ST2 blockade elicited expansion of intestinal MDSCs (CD45.1$^+$ MAC-1$^+$Gr-1$^+$) in anti-ST2 mAb–treated mice (Fig. 4A). Recipients receiving ST2$^{-/-}$ donor T cells also showed significantly increased frequencies of intestinal MDSCs. In addition, given that intestinal CD103$^+$ dendritic cells have been shown to generate $\alpha_4\beta_7$ gut-tropic effector T cells in the intestine and MLNs (*28*), we measured the frequencies of these cells in our GVHD model with and without treatment. The frequencies of CD103$^+$ dendritic cells were reduced after ST2 blockade in the GI tract (Fig. 4C) and MLNs (fig. S5). Similar results were observed in mice receiving ST2$^{-/-}$ donor T cells (Fig. 4D). The total CD11c$^+$ dendritic

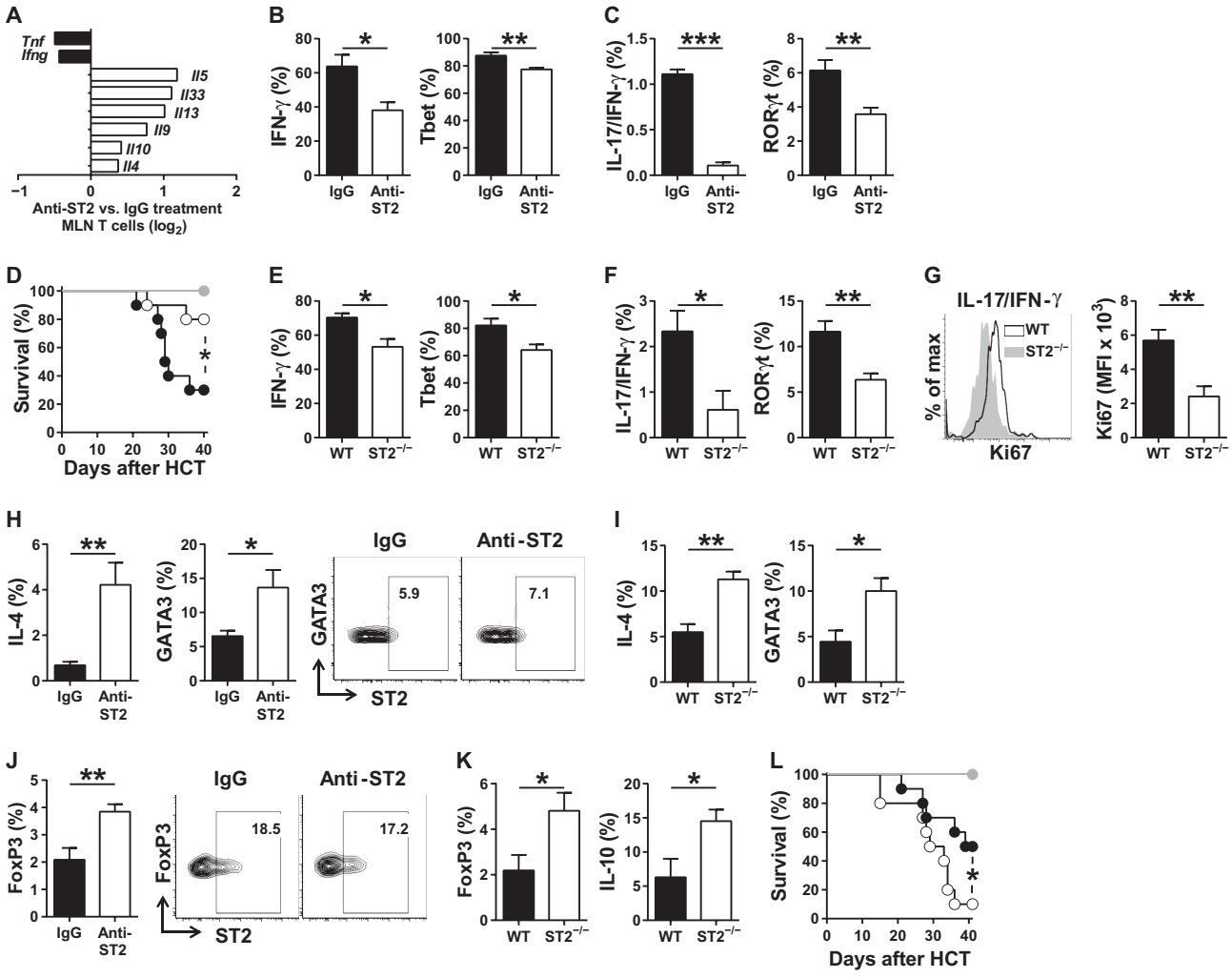

Fig. 3. ST2 deficiency and T cell populations during GVHD. (**A**) Transcriptome analysis of T cell–related genes in MLN T cells from anti-ST2–treated versus IgG-treated C3H.SW recipient mice at day 10 after allo-HCT. MLN T cells from four mice in each group were pooled for analysis. (**B** and **C**) Flow cytometric analysis of transcription factor and cytokine production by donor-derived $CD4^+$ splenic T cells from IgG-treated or anti-ST2–treated C3H.SW recipient mice at day 10 after allo-HCT. The bar graphs show the percentages of cells expressing IFN-γ or Tbet ($P = 0.0150$ for IFN-γ and $P = 0.0055$ for Tbet, *t* test; $n = 5$) (B) and IL-17/IFN-γ or RORγt ($P = 0.0003$ for IL-17/IFN-γ and $P = 0.0075$ for RORγt, *t* test; $n = 4$ to 5) (C). The data are from two independent experiments. Gating strategy for (B) and (C) is found in fig. S10. (**D**) Survival curves for C3H.SW recipient mice receiving either only 5×10^6 wild-type (WT) B6 BM cells (—●—) or 2×10^6 WT (—●—) or $ST2^{-/-}$ B6 T cells (—○—) ($P = 0.0289$, log-rank test; $n = 6$ to 10). The data are from two independent experiments. (**E** to **G**) Flow cytometric analysis at day 10 after allo-HCT shows percentages of intestinal $CD4^+$ T cells expressing IFN-γ and Tbet ($P = 0.0173$ for IFN-γ and $P = 0.0320$ for Tbet, *t* test; $n = 4$) (E) and IL-17/IFN-γ and RORγt ($P = 0.0273$ for IL-17/IFN-γ and $P = 0.0273$ for RORγt, *t* test; $n = 4$ to 5) (F) as well as Ki67 proliferation staining of cells expressing both IL-17 and IFN-γ ($P = 0.0088$, *t* test; $n = 4$) (G). The data are from two independent experiments. MFI, mean fluorescence intensity. (**H**) The bar graphs show the percentages of T cells expressing IL-4 or GATA3 from IgG-treated or anti-ST2–treated C3H.SW recipient mice at day 10 after allo-HCT, and the flow cytometry plots show mST2 expression on GATA3 T cells after IgG or anti-ST2 treatment. The data are from two independent experiments ($P = 0.0049$ for IL-4 and $P = 0.0252$ for GATA3, *t* test; $n = 6$). (**I**) IL-4– and GATA3-expressing T cells from C3H.SW recipient mice receiving WT or $ST2^{-/-}$ B6 T cells at day 10 after allo-HCT ($P = 0.0032$ for IL-4 and $P = 0.0253$ for GATA3, *t* test; $n = 4$). The data are from two independent experiments. (**J**) The bar graphs show the percentages of intestinal T cells expressing FoxP3 from IgG-treated or anti-ST2–treated C3H.SW recipient mice at day 10 after allo-HCT, and the flow cytometry plots show mST2 expression on FoxP3 T cells after IgG or anti-ST2 treatment ($P = 0.0087$, *t* test; $n = 5$). The data are from two independent experiments. (**K**) FoxP3- and IL-10–expressing T cells from C3H.SW recipient mice receiving WT or $ST2^{-/-}$ B6 T cells at day 10 after allo-HCT. The data are from two independent experiments ($P = 0.0459$ for FoxP3 and $P = 0.0471$ for IL-10, *t* test; $n = 4$ to 5). (**L**) Survival curves for C3H.SW recipient mice transplanted with 5×10^6 B6 TCD BM cells plus 2×10^5 WT (—●—) or $ST2^{-/-}$ B6 (—○—) T_{regs} with 2×10^6 WT B6 T_{conv} cells. (—●—, TCD BM only). The data are from two independent experiments ($P = 0.043$, log-rank test; $n = 5$ to 10 per group). Flow cytometric gating strategies are shown in fig. S10.

cells from treated animals showed reduced expression of MHC class II and costimulatory molecules (CD40, CD80, and CD86) on their surface as compared to the control group (Fig. 4E). Mast cells that express mST2 have been shown to play a major role in supporting T_{regs} in several diseases including GVHD (*29*, *30*). However, using the classical c-kit and FcεRI markers, we could not identify intestinal mast cells during GVHD (fig. S4C).

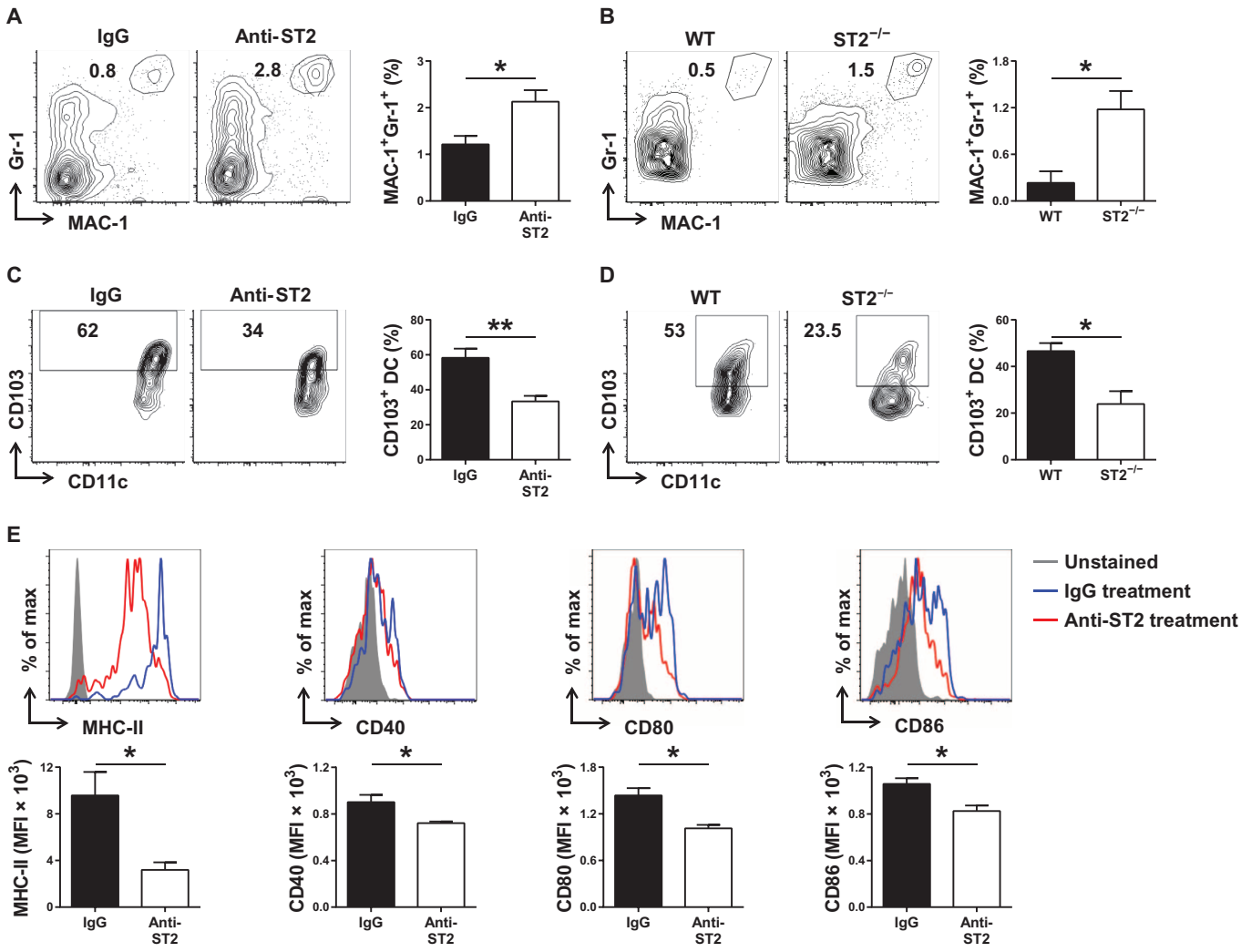

Fig. 4. ST2 deficiency and antigen-presenting cells during GVHD. Flow cytometric analysis of intestinal MDSCs (MAC-1$^+$Gr-1$^+$ cells), CD103$^+$ dendritic cells, and CD11c$^+$ total dendritic cells in the B6 (CD45.1$^+$)→C3H.SW (CD45.2$^+$) model at 10 days after allo-HCT. (**A**) Donor CD45.1$^+$ MDSCs in IgG control– or anti-ST2–treated C3H.SW recipients (P = 0.0247, t test; n = 4). The data are from two independent experiments. (**B**) Donor CD45.1$^+$ MDSCs in C3H.SW recipients receiving WT or ST2$^{-/-}$ B6 T cells (P = 0.0277, t test; n = 3). (**C**) Donor CD45.1$^+$CD103$^+$ dendritic cells (DC) in IgG control– or anti-ST2–treated C3H.SW recipients (P = 0.0012, t test; n = 8). The data are from four independent experiments. (**D**) Donor CD45.1$^+$CD103$^+$ dendritic cells in C3H.SW recipients receiving WT or ST2$^{-/-}$ B6 T cells (P = 0.0244, t test; n = 3). (**E**) Expression of MHC class II and costimulation molecules on CD11c$^+$ total dendritic cells from IgG control– and anti-ST2–treated mice, representative flow cytometry histograms (top panels), and bar graphs (bottom panels) of MFI (P = 0.0391 for MHC class II, P = 0.0469 for CD40, P = 0.0154 for CD80, and P = 0.0263 for CD86, t test; n = 3). Flow cytometric gating strategies are shown in fig. S11.

ST2 blockade preserves substantial antitumoral cytotoxicity and GVL activity

Due to the strong effect of anti-ST2 mAb blockade on not only stromal/endothelial cells but also T cells, it was crucial to verify that the T cell antitumoral cytotoxicity and GVL activity were preserved. One indication that GVL activity was preserved was the up-regulation of cytokines and cytolytic molecules that have been implicated in antitumoral or GVL activity, such as IL-27 (*31*, *32*), IL-18 (*33*), IL-9 (*34*, *35*), type I IFNs (*36*), and granzyme A (*37*), in T cells from the MLNs in anti-ST2 mAb–treated versus nontreated animals (Fig. 5A). In vitro cytolytic assays were performed against syngeneic tumors [A20 lymphoma cells and enhanced GFP (eGFP)–positive MLL-AF9 leukemic cells] after stimulation of allogeneic antigen with a mixed lymphocyte reaction. Addition of anti-ST2 mAb did not decrease antitumoral cytotoxicity (Fig. 5B). Furthermore, because of two major limitations of current GVL models, the first being the use of models that overestimate CD4-dependent pathways relative to those observed clinically and the second being the use of cell lines that are extremely sensitive to GVL activity (*5*), we developed primary retrovirally induced eGFP$^+$ MLL-AF9 leukemic cells on the C3H.SW background. The phenotype of the leukemic cells in this model is eGFP$^+$, CD3$^-$, B220$^-$, and MAC-1^{hi}Gr-1^{hi} and is based on previous reports (*38*, *39*). Our results indicate that administration of anti-ST2 mAb over a short course (2 days, Fig. 5C) or a long course (6 days, Fig. 5D) or of ST2$^{-/-}$ donor T cells (Fig. 5E) preserved substantial GVL activity and resulted in significantly improved leukemia-free survival.

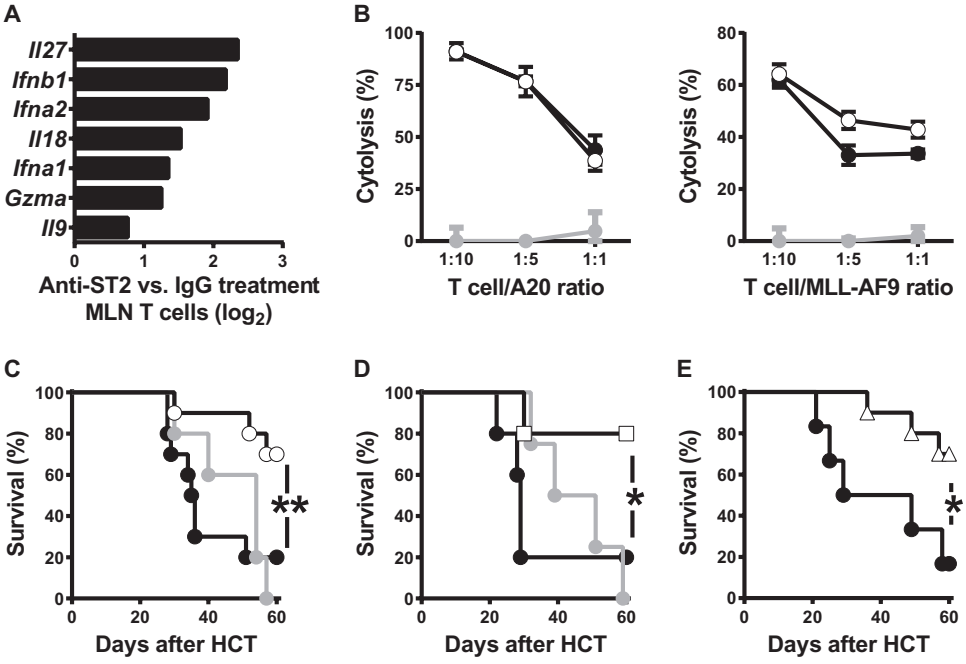

Fig. 5. ST2 deficiency and GVL activity. (**A**) Transcriptome analysis of antitumor-related genes in MLN T cells from anti-ST2–treated versus IgG-treated C3H.SW recipient mice at day 10 after allo-HCT. MLN T cells from four mice in each group were pooled for analysis. (**B**) In vitro cytotoxic T lymphocyte assay with A20 and MLL-AF9 retrovirally induced acute myeloid leukemia in the presence of IgG control (●) and anti-ST2 mAb (○) (5 μg/ml). Syngeneic control (●) ($n = 3$). The data are from three independent experiments. (**C**) Survival curves of C3H.SW mice receiving 10^4 GFP$^+$ MLL-AF9 leukemic cells with syngeneic HCT C3H.SW→C3H.SW (●) or allo-HCT (B6→C3H.SW) treated with IgG control (●) or anti-ST2 mAb (○) ($P = 0.010$, log-rank test; n = 5 to 10 per group). (**D**) Survival curves of C3H.SW mice receiving 10^4 GFP$^+$ MLL-AF9 leukemic cells with syngeneic HCT C3H.SW→C3H.SW (●) or allo-HCT (B6→C3H.SW) treated with six doses (100 μg per dose, every other day from day −1 to day +9) of IgG control (●) or anti-ST2 mAb (□) ($P = 0.0357$, log-rank test; n = 4 to 5 per group). (**E**) Survival curves of C3H.SW mice receiving 10^4 GFP$^+$ MLL-AF9 leukemic cells with WT (●) or ST2$^{-/-}$ (△) B6 T cells ($P = 0.0203$, log-rank test; n = 6 to 10 per group).

DISCUSSION

Pharmacological interventions are required to harness the therapeutic potential of sST2 inhibition. Here, we report that inhibition strategies using anti-ST2 mAb (*26*) reduced the severity of acute GVHD as well as GVHD mortality in the B6→C3H.SW and human T cell→NSG experimental murine model. Transient ST2 inhibition achieved with two doses of mAb was sufficient to provide long-lasting protection against GVHD. As hypothesized, blockade of the decoy receptor decreased circulating IFN-γ, IL-17, and IL-23 levels and released systemic IL-10 and IL-33 levels.

IL-33 has a paradoxical role in immune responses depending on the inflammatory environment and cell types involved. For example, it has recently been shown that IL-33 can increase the function of colonic ST2$^+$ T$_{regs}$ in a colitis model (*25*) and can exacerbate allergic bronchoconstriction through activation of ST2$^+$ mast cells in a mouse model of allergy (*40*). IL-33 has also been shown to synergize with IL-12 to activate natural killer and natural killer T cells and to enhance their IFN-γ production (*41*). A recent study showed that exogenous IL-33 administration during the cytokine storm worsened GVHD (*42*). In our models, adding exogenous IL-33 (five injections in the peritransplantation period) had no worsening or protective effect on GVHD (fig. S6). This might be due to the fact that in our minor mismatched models, lower levels of inflammatory cytokines are secreted in response to conditioning and alloreactivity as compared to levels in major mismatched models. On the contrary, we demonstrated an increase in systemic IL-10 and IL-33 that indirectly inhibited the expansion of pathogenic T cells and the production of inflammatory cytokines such as IFN-γ, IL-17, and IL-23. We also demonstrated that anti-ST2 mAb formed a stable complex with sST2 in circulating blood that could be released by immunodepletion of the immune complexes confirming that anti-ST2 mAb can specifically inhibit sST2 (fig. S7). The significant increases in plasma sST2 levels in miHA-mismatched allo-HCT and human-to-mouse xenogeneic experimental models by days 10 and 20 (time of human T cell engraftment) after transplantation, respectively, mimicked the kinetics observed in patients (*10*). These kinetics in plasma sST2 as well as plasma inflammatory and anti-inflammatory cytokines may have important clinical implications. The ability to identify high-risk patients by measuring plasma concentrations of sST2 and other systemic cytokines as early as day 14 after transplantation, before the development of GVHD, may allow more stringent monitoring and preemptive interventions based on these markers and the use of a GVHD-specific inhibitor.

Although it was previously shown using the technologies available at the time that activated CD4$^+$ T cells, but not resting T cells, might produce sST2 while expressing low levels of mST2 (*43*), this has never been demonstrated in the context of diseases through extensive analysis of all T cell subsets. We have shown here that there is a differential balance of sST2 secretion versus mST2 expression in alloreactive T cells. Indeed, with increasing severity of GVHD, more pathogenic T cells (T$_H$17 and T$_c$17) secrete sST2 and express less mST2, possibly explaining why elevation of plasmatic sST2 is specific to alloreactivity. This study also emphasizes that T$_H$17 and T$_c$17 cells are mainly seen in the intestine during GVHD and are important players in GVHD development. We have clearly shown that transient ST2 blockade specifically inhibited sST2 in the plasma and target organs, particularly in the GI tract, while maintaining the mST2 expression on T cells, particularly T$_H$2 and ST2$^+$ T$_{regs}$.

We also found that ST2 blockade not only decreased the expression of the T$_H$1 transcription factor Tbet and the corresponding inflammatory cytokine IFN-γ but also increased the production of the T$_H$2 transcription factor GATA3 and the T$_H$2 cytokine IL-4, skewing the T$_H$1/T$_H$2 balance toward a T$_H$2 phenotype, which protects against severe GVHD. In addition, we and others have previously shown that the ratio of FoxP3-expressing T$_{regs}$ to conventional T cells is significantly decreased in severe GVHD (*44*–*46*). ST2 blockade also increased the

frequency of functional FoxP3$^+$ T_{regs} in the spleen and gut and decreased the percentage of pathogenic T_H17 cells, without impairing the ST2$^+$FoxP3$^+$ T_{regs} that we showed are crucial for protection against GVHD. Because the anti-ST2 mAb used in our study is a full-length antibody that potentially inhibits both the soluble and membrane-bound forms, we verified that the inhibitory effect was limited to the soluble form by measuring the frequency of ST2$^+$ T_{regs} after treatment. In accordance with the findings of a recent study showing that ST2$^+$ T_{regs} have a better suppressive capacity than T_{regs} not expressing mST2 and are better able to prevent colonic inflammation (*25*), we confirmed that this is true in intestinal GVHD as well. Indeed, ST2$^{+/+}$ T_{regs} more effectively protected against GVHD than ST2$^{-/-}$ T_{regs}. However, we demonstrated that although ST2$^{+/+}$ T_{regs} have an important protective role in GVHD, the role of sST2 secretion by alloreactive T_{conv} is predominant because HCT with ST2$^{-/-}$ donor T_{conv} with or without ST2$^{+/+}$ donor T_{regs} (T_{regs}/T_{conv} ratio of 1:10) resulted in less severe GVHD and improved survival in both cases (fig. S8, table S3, and Fig. 3D). Together, our results indicate that high levels of sST2 production by T cells during GVHD may represent a mechanism to further perpetuate pathogenic responses by limiting IL-33–driven T_{reg} accumulation.

T cell subsets are regulated by antigen-presenting cells. Given the role of the ST2/IL-33 pathway in MDSCs and mast cells (*21*, *22*, *29*, *30*), we explored their respective frequencies as well as that of CD103$^+$ dendritic cells in the intestine and MLNs during GVHD with and without ST2 deficiency. ST2 deficiency (ST2 blockade or knockout) induces expansion of tolerogenic MDSCs and a decrease in CD103$^+$ dendritic cells. Furthermore, the total CD11c$^+$ dendritic cells from treated animals expressed lower levels of MHC class II and costimulatory molecules (CD40, CD80, and CD86) on their surface as compared to the control group. The potential mechanisms responsible for these changes need to be further explored.

The GI tract has been shown to be the sentinel site for GVHD (*47*), and this may be due to the presence of large numbers of nonhematopoietic stromal cells that can act as antigen-presenting cells in this target organ (*48*). GVHD of the GI tract affects up to 60% of HCT recipients, and the GI tract is also the GVHD target organ associated with the highest mortality rate (*49*, *50*). Consistent with the tropism of GVHD for the GI tract, we found that the intestine was indeed the major source of sST2, particularly the stromal cells and endothelial cells of the GI tract, which are classically damaged during conditioning by irradiation or chemotherapy. We further confirmed the importance of host sST2 in GVHD based on the observation of less severe GVHD in recipient ST2$^{-/-}$ mice. We also demonstrated that intestinal T cells are another major source of sST2. This mechanism whereby sST2 is secreted mainly by CD4$^+$ T cells (mostly T_H17 cells) may explain the specificity of sST2 immune functions during alloreactivity as well as the marked protective effect of anti-ST2 blockade on GVHD severity and mortality. Indeed, our findings highlight the therapeutic potential of targeting sST2 as a new strategy for controlling GVHD after allo-HCT, which could be applied in a number of other diseases with elevated sST2 that are commonly due to T cell dysregulation in immune responses.

Finally, ST2 blockade retained substantial GVL activity. The reasons might be that (i) Tbet$^+$ and IFN-γ$^+$ CD4 T cells are suppressed to a lesser extent after ST2 blockade (Fig. 3A); (ii) anti-ST2 mAb may target more specifically alloreactive sST2-producing T cells that are not implicated in GVL activity; (iii) cytokines and cytolytic molecules related to antitumoral or GVL activity are up-regulated in mice treated with anti-ST2 mAb (Fig. 5A).

Several limitations to the present study should be noted. First, although ST2 blockade ameliorates GVHD mortality in correlation with an increase in systemic IL-33, ex vivo systemic injections of IL-33 did not lead to improvement in the treated animals, suggesting that endogenously produced IL-33 and exogenously administered IL-33 have different (i) circulating doses (in the pg/ml range versus ng/ml range, respectively), (ii) pharmacokinetics, and (iii) binding properties in vivo. Second, the anti-ST2 mAb from Centocor recognizes both sST2 and mST2, which may target the beneficial effect of ST2$^+$ T_{regs}. Although we have demonstrated that (i) sST2 during GVHD was produced by the key T cell players, (ii) that ST2$^+$ T_{regs} were not decreased, and (iii) that the net result of ST2 blockade was GVHD alleviation, the development of mAbs or small inhibitory molecules targeting only sST2, leaving mST2 intact, would further strengthen the results found in our study. Furthermore, an ST2-Fc fusion protein has been developed and used with some success to inhibit ST2/IL-33 signaling in vitro (*51*) and in vivo (*42*). mAbs will need to be humanized for use in clinical trials. Third, we have only shown the protective effect of ST2 blockade when used as a prophylactic treatment; thus, further experiments are needed to show the effects of ST2 blockade in models in which acute GVHD has already started to develop and in chronic GVHD models.

In summary, our findings identify intestinal alloreactive T cells as an important source of the decoy receptor for IL-33 that can be blocked with two doses of anti-ST2 mAb in the peritransplant period without inhibiting the beneficial mST2 expression on T_H2 cells and T_{regs}. This study offers new perspectives on the translation of drug-targetable biomarkers for selectively and safely treating GVHD and other T cell–mediated human disorders.

MATERIALS AND METHODS

Study design

This study was designed to inhibit the interaction between IL-33 and sST2, the decoy receptor for IL-33, to release free IL-33 as a proof-of-principle demonstration of a drug-targetable biomarker. We assessed the potential of sST2 blockade in multiple experimental models of GVHD. We used an anti-ST2 mAb from Centocor (CNT03914), which was available to us through a material transfer agreement, or an appropriate control isotype antibody (IgG) with different doses and schedules. We evaluated the therapeutic effect of anti-ST2 mAb in GVHD by monitoring GVHD clinical scores, histopathological GVHD scores, and survival. We also measured the increases in production of the systemic anti-inflammatory cytokines IL-10 and IL-33 and the decreases in systemic proinflammatory cytokine production by ELISA. We then investigated the source of sST2 during GVHD by analyzing sST2 secretion in different organs. We further assessed the ratio of sST2-secreting T cells to mST2-expressing T cells, mostly FoxP3$^+$ T_{regs}. We also compared the protective effects of mST2-expressing T_{regs} and ST2$^{-/-}$ T_{regs} against GVHD. Finally, we generated a model of retrovirally transduced GFP$^+$ MLL-AF9 acute myeloid leukemia to assess the effects of ST2 blockade on GVL activity. All experiments were replicated at least three times.

Mice

Balb/c (H-2^d), B6 (H-2^b, CD45.2$^+$), B6 (C57BL/6.Ptprca, H-2^b, CD45.1$^+$), C3H.SW (H-2^b, CD45.2$^+$), and NSG mice were from The

Jackson Laboratory. B6 ($ST2^{-/-}$, H-2^b, CD45.2^+) mice were provided by A. McKenzie from University of Cambridge, UK. B6 ($ST2^{-/-}$, H-2^b, CD45.1^+) mice were bred in the mouse breeding facility at Indiana University School of Medicine. Animal protocols were approved by the Institutional Animal Care and Use Committee at Indiana University School of Medicine.

Induction and assessment of GVHD

The mice underwent allo-HCT as previously described (*52*). Briefly, in miHA-mismatched GVHD models (B6→C3H.SW and C3H.SW→B6), C3H.SW or B6 recipient mice received 1100 and 1250 cGy of total body irradiation (^{137}Cs as source) at day −1. Then, recipient mice were injected intravenously with T cell–depleted (TCD) BM cells (5×10^6) plus splenic T cells (2×10^6 for C3H.SW, 3×10^6 for B6) from either syngeneic or allogeneic donors at day 0. T cells from donor mice were enriched using the murine Pan T Cell Isolation Kit (Miltenyi), and TCD BM was prepared with CD90.2 Microbeads (Miltenyi). For adoptive transfer models (B6→C3H.SW), wild-type and $ST2^{-/-}$ B6 total donor T cells or T_{regs} were purified using the murine Pan T Cell Isolation Kit and murine $CD4^+CD25^+$ Regulatory T Cell Isolation Kit (Miltenyi). Irradiated C3H.SW recipient mice were injected intravenously with TCD BM cells (5×10^6) and the indicated number of T cells in different experiments. In the xenogeneic GVHD model (human T cells→NSG mice), irradiated (350 cGy) NSG mice were transplanted with total human T cells from PBMCs (2.5×10^6) at day 0. PBMCs were prepared from human PB Leukopacks from healthy donors, which were purchased from the Central Indiana Blood Center under an Institutional Review Board–approved protocol. PBMCs were isolated within 24 hours after blood draw by Ficoll density gradient centrifugation (GE Healthcare). Total human T cells were purified using the human Pan T Cell Isolation Kit (Miltenyi). The mice were housed in sterilized microisolator cages and maintained on acidified water (pH <3) for 3 weeks as previously described (*53*). NSG mice were maintained on food supplemented with Uniprim and acid water during the whole time course of the experiment. Survival was monitored daily. Clinical GVHD scores were assessed weekly as previously described (*54*). According to animal protocols approved by the Institutional Review Board, mice were euthanized when the clinical score achieved 6.5.

ELISA

Concentrations of ST2 (both murine and human), IL-17A, IL-23, and IL-33 in mouse plasma and culture supernatants were measured with the Quantikine ELISA Kits (R&D Systems). IFN-γ and IL-10 were measured with the DuoSet ELISA Kit (R&D Systems).

Anti-ST2 mAb treatment

The anti-ST2 mAb was from Centocor, a pharmaceutical company of Johnson & Johnson (CNT03914). This chimeric antibody contains a mouse IgG1 Fc, and it recognizes the full-length extracellular domain of mST2 (*26*). Anti-ST2 mAb or IgG control antibody was given to recipient mice receiving allo-HCT mice via intraperitoneal injection at day −1 and day 1 after HCT, at 100 μg per mouse. In some experiments, the mice received six doses of anti-ST2 mAb every other day from day −1 to day +9. In the xenogeneic GVHD model, NSG mice received four doses of both anti-human (clone 97203, R&D Systems) and anti-mouse ST2 (CNT03914) mAbs every other day from day −1 to day 5 (intraperitoneally, 100 μg per mouse).

Histopathological analysis of GVHD

Specimens of liver and intestine were made of formalin-preserved tissue by the Pathology Department at Indiana University Medical Center. The slides were coded without reference to previous treatment and examined in a blinded fashion by C. Liu (University of Florida). A semiquantitative scoring system was used to assess abnormalities known to be associated with GVHD (*55*, *56*). After scoring, the codes were broken and the data were compiled.

Isolation of intestinal cells

Single-cell suspensions were prepared from intestines as described, with modifications (*57*). Briefly, intestines were flushed with phosphate-buffered saline to remove fecal matter and mucus. Fragments (<0.5 cm) of intestines were digested in 10 ml of Dulbecco's modified Eagle's medium (DMEM) containing collagenase type B (2 mg/ml) (Roche), deoxyribonuclease I (10 μg/ml) (Roche), and 4% bovine serum albumin (Sigma) at 37°C with shaking for 90 min. The digested mixture was then diluted with 30 ml of plain DMEM, filtered through 70-μm strainers, and centrifuged at 850*g* for 10 min. The cell pellets were suspended in 5 ml of 80% Percoll (GE Healthcare), overlaid with 8 ml of 40% Percoll, and spun at 2000 rpm for 20 min at 4°C without braking. Enriched lymphocytes were collected from the interface. Stromal, endothelial, epithelial, and $CD45^+TCR\beta^-$ cells were directly sorted from single-cell suspensions without Percoll separation.

Flow cytometric analysis and cell sorting

All antibodies (table S4) and reagents for flow cytometry were purchased from eBioscience, unless stated otherwise. The cells were preincubated with purified anti-mouse CD16/CD32 mAb for 10 to 20 min at 4°C to prevent nonspecific binding of the antibodies. The cells were subsequently incubated for 30 min at 4°C with antibodies for surface staining. Fixable viability dye (FVD) was used to distinguish live cells from dead cells. The FoxP3/Transcription Factor Staining Buffer Set and the Fixation and Permeabilization Kit were used for intracellular transcription factor and cytokine staining. For cytokine staining, cells were restimulated with phorbol myristate acetate (PMA; 50 ng/ml), ionomycin (1 μg/ml; Sigma-Aldrich), and brefeldin A for 4 to 6 hours before any staining.

Cell sorting

MLN T cells [$FVD^-CD90.2^+CD3^+$] from treated C3H.SW recipient mice receiving allo-HCT were sorted for nanostring analysis. Total T cells ($FVD^-CD45^+TCR\beta^+$), $CD4^+$ T cells, $CD8^+$ T cells, $CD45^+TCR\beta^-$ cells, stromal cells ($FVD^-CD45^-EpCAM^-$), epithelial cells ($FVD^-CD45^-EpCAM^+$), and endothelial cells ($FVD^-CD45^-EpCAM^-$ $CD146^+$) were sorted from single-cell suspensions of intestine from treated C3H.SW recipient mice for quantitative reverse transcription polymerase chain reaction (RT-PCR) or Western blot analysis. Cell sorting was performed on BD FACSAria (BD Bioscience) or iCyt Reflection (Sony Biotechnology) in the flow cytometry core facility at Indiana University School of Medicine.

Nanostring analysis

Sorted MLN T cells from either IgG control– or anti-ST2 mAb–treated GVHD mice were directly lysed in RLT buffer (Qiagen) on ice. The cell concentration for lysis was 0.2×10^4 to 1×10^4 cells/μl in a total volume of 5 μl with RLT buffer. Lysis samples were immediately frozen in liquid nitrogen and then stored at −80°C or in dry ice. Nanostring

analysis was performed with the nCounter Analysis System at NanoString Technologies. The nCounter Mouse Immunology Kit, which includes 561 immunology-related mouse genes, was used in the study.

Quantitative RT-PCR

Total RNA from spleen, small intestine, large intestine, skin, BM, lung, heart, and peripheral blood were isolated using the RNeasy Plus Mini Kit (Qiagen). Complementary DNA (cDNA) was prepared with the SuperScript VILO cDNA Synthesis Kit (Invitrogen). Quantitative real-time PCR was performed using SYBR Green PCR mix on an ABI Prism 7500HT (Applied Biosystems). Thermocycler conditions included 2-min incubation at 50°C, then at 95°C for 10 min; this was followed by a two-step PCR program: 95°C for 5 s and 60°C for 60 s for 40 cycles. β-Actin was used as an internal control to normalize for differences in the amount of total cDNA in each sample. The primer sequences were as follows: actin forward, 5′- CTCTGGCTCCTAGCACCATGAAGA-3′ (*58*); actin reverse, 5′- GTAAAACGCAGCTCAGTAACAGTCCG-3′; mST2 forward, 5′-AAGGCACACCATAAGGCTGA-3′;mST2 reverse, 5′-TCGTAGAGCTTGCCATCGTT-3′; sST2 forward, 5′-TCGAAATGAAAGTTCCAGCA-3′ (*25*); sST2 reverse, 5′-TGTGTGAGGGACACTCCTTAC-3′.

Two-color Western blots

Sorted cells were lysed in RIPA (radioimmunoprecipitation assay) buffer (Pierce Biotechnology) with Pierce Phosphatase Inhibitor Mini Tablets (Pierce Biotechnology) and Protease Inhibitor Cocktail Tablets (Roche). Samples were boiled, electrophoretically separated, and transferred on Immobilon-FL polyvinylidene difluoride membranes (Millipore). The blots were blocked with Odyssey Blocking Buffer (LI-COR) for 1 hour at room temperature and incubated with specific primary antibodies: biotinylated anti-mouse ST2 mAb (DJ8, MD Bioproducts) and anti–β-actin mAb (926-42212, LI-COR), at 4°C overnight. IRDye 800CW streptavidin (926-32230, LI-COR) and IRDye 680RD goat anti-mouse IgG polyclonal antibodies (926-68070, LI-COR) were used as secondary detection antibodies for ST2 and β-actin, respectively. Fluorescence from blots was then developed with the Odyssey CLx Imaging System (LI-COR) according to the manufacturer's instructions.

T cell differentiation

Total $CD4^+$ or $CD8^+$ T cells were purified from B6 spleens with magnetic isolation beads (Miltenyi). These cells were plated at a concentration of 1×10^6 cells/ml and activated with plate-bound anti-CD3 (2C11) (1 μg/ml) and soluble anti-CD28 (37.51) (5 to 10 μg/ml). Both the $CD4^+$ and $CD8^+$ cells were polarized toward either T_H1/T_c1 [IL-2 (1 ng/ml) and IL-12 (20 ng/ml)], T_H2/T_c2 [IL-4 (20 ng/ml)], or T_H17/T_c17 [transforming growth factor–β (TGF-β) (4 ng/ml), IL-6 (10 ng/ml), IL-1β (10 ng/ml), and IL-23 (20 ng/ml)] conditioning in complete medium. On day 3, the cells were expanded with fresh medium in the presence of additional cytokines at the same concentration as on day 0 for T_H1/T_c1, T_H2/T_c2, and T_H17/T_c17 cells. On day 5, the cells were stimulated with anti-CD3 and anti-CD28 (both 10 μg/ml) as well as with PMA (50 ng/ml) and ionomycin (1 μg/ml) overnight. The next day, the supernatant was collected for ELISA analysis. Cytokines and antibodies were purchased from R&D Systems (IL-1β, IL-2, IL-4, IL-6, IL-12, IL-23, and TGF-β) and eBioscience (anti-CD3 and anti-CD28). Human T cells were purified from PBMCs of healthy donors and activated with anti-CD3/CD28 microbeads (anti-CD3/ICOS for T_H17/T_c17) from Life Technologies. Both the $CD4^+$ and $CD8^+$ cells were polarized toward either T_H1/T_c1 [IL-2 (1 ng/ml), IL-12 (20 ng/ml), and anti–IL-4 (10 μg/ml)], T_H2/T_c2 [IL-4 (20 ng/ml) and anti–IFN-γ(10 μg/ml)], or T_H17/T_c17 [TGF-β (4 ng/ml), IL-6 (10 ng/ml), IL-1β (10 ng/ml), IL-23 (20 ng/ml), anti–IL-4 (10 μg/ml), and anti–IFN-γ (10 μg/ml)] conditioning in complete medium. On day 3, the cells were expanded with fresh medium in the presence of additional cytokines at the same concentration as on day 0 for T_H1/T_c1, T_H2/T_c2, and T_H17/T_c17 cells. On day 7, the cells were stimulated with anti-CD3 and anti-CD28 (both 10 μg/ml) as well as with PMA (50 ng/ml).

Generation of MLL-AF9-eGFP leukemic cells

The retroviral vector containing the MLL-AF9 eGFP cDNA construct (*38*) was provided by R. Kapur and used to generate retroviral supernatants by transit transfection of Phoenix-Eco Cell Line (ATCC) using FuGENE 6 transfection reagent (Promega). Eighteen hours before transfection, Phoenix-Eco cells were seeded in gelatin-coated 100-mm plates (8×10^6 per plate). After gently aspirating off the cell culture medium, the cells were transfected with a mixture of 20 μg of DNA and 60 μl of transfection reagent (3 μl/μg DNA) in 5 ml of plain DMEM. After 6 to 8 hours, 3 ml of DMEM supplemented with 15% heat-inactivated fetal bovine serum (FBS) was added to the plates. After 18 hours of incubation, the medium was replaced with 8 ml of Iscove's modified Dulbecco's medium (Life Technologies) supplemented with 10% FBS, penicillin and streptomycin (100 U/ml), and 1 mM sodium pyruvate. After a 24-hour incubation, retroviral supernatants were collected and filtered through 0.45-μm filters. Freshly prepared retroviruses were used to transduce c-kit^+ cells that were magnetically enriched from Balb/c or C3H.SW BM cells using the CD117 MicroBead Kit (Miltenyi) and were prestimulated for 48 hours with IL-3 (10 ng/ml), IL-6 (10 ng/ml), and stem cell factor (20 ng/ml) (all from PeproTech). After two consecutive 24-hour infections in nontissue culture plates precoated with retronectin (*59*), the cells were collected and their infection efficiency was determined by eGFP expression, using flow cytometry. About 1×10^6 of cells, 8% of which were $eGFP^+$, were injected into lethally irradiated Balb/c or C3H.SW mice intravenously through the tail vein. The mice were monitored daily and checked weekly for leukemia development through total blood cell and platelet counts (Hemavet 1700, Drew Scientific). At day 35, mouse peripheral blood showed high leukocyte counts, anemia, and low platelet counts (leukemia symptoms). The mice were subsequently euthanized, and BM cells were analyzed by flow cytometry, which showed that all BM cells were $eGFP^+$, $CD3^-$, $B220^-$, and MAC-1^{hi}Gr-1^{hi}.

In vitro cytotoxicity assay

The A20 cell line expressing E2-Crimson fluorescent protein was provided by H. Hanenberg. Cytotoxicity assays were performed as previously described (*34*, *35*), with some modifications. Briefly, T cells were primed in a mixed lymphocyte reaction. E2-Crimson A20 or eGFP-expressing MLL-AF9 cells were incubated with syngeneic Balb/c or allogenic B6 T cells at different ratios as indicated. After 8 hours of incubation at 37°C, the cells were analyzed by flow cytometry.

Induction and assessment of GVL effect

C3H.SW mice were lethally irradiated (1100 cGy) 1 day before BM transplantation. Recipient mice were injected intravenously with 5×10^6 B6 or C3H.SW BM cells, 2×10^6 enriched B6 or C3H.SW splenic T cells, and 10^4 MLL-AF9 cells on day 0. The mice were treated

intraperitoneally with anti-ST2 antibody or isotype IgG control at day −1 and day +1 or with six doses of anti-ST2 mAb every other day from day −1 to day +9, as described above. The mice were monitored daily for survival and leukemia development and weekly for GVHD score. We attributed death to leukemia on the basis of a high percentage of eGFP$^+$ cells and death to GVHD only if the mice had a low percentage of eGFP$^+$ cells and a GVHD score of 6.5. Cells from peripheral blood, BM, spleen, and liver were analyzed by flow cytometry.

Statistics

Log-rank test was used for survival analysis. Differences between two groups were compared using unpaired *t* test with GraphPad Prism software, version 6.05. Error bars in graphs represent mean ± SEM. Differences between three or more groups were compared using one-way ANOVA followed by Dunnett's multiple comparisons test using GraphPad Prism software, version 6.05. *P* values less than 0.05 were considered significant.

SUPPLEMENTARY MATERIALS

www.sciencetranslationalmedicine.org/cgi/content/full/7/308/308ra160/DC1
Materials and Methods
Fig. S1. Six dose ST2 blockade and GVHD.
Fig. S2. Host ST2 deficiency and GVHD.
Fig. S3. mST2 expression on T cell subsets.
Fig. S4. Antigen-presenting cells and GVHD.
Fig. S5. MLN dendritic cells and GVHD.
Fig. S6. IL-33 administration and GVHD.
Fig. S7. Immune complex depletion.
Fig. S8. ST2 deficiency in T_{conv} cells and GVHD.
Fig. S9. Unmodified blots.
Fig. S10. Gating strategies of flow cytometric analysis for Fig. 3.
Fig. S11. Gating strategies of flow cytometric analysis for Fig. 4E.
Table S1. *P* values for Fig. 1.
Table S2. *P* values for Fig. 2.
Table S3. *P* values for figs. S1, S2, and S8.
Table S4. Antibodies for flow cytometry.

REFERENCES AND NOTES

1. C. J. Wu, J. Ritz, Induction of tumor immunity following allogeneic stem cell transplantation. *Adv. Immunol.* **90**, 133–173 (2006).
2. H. J. Kolb, Graft-versus-leukemia effects of transplantation and donor lymphocytes. *Blood* **112**, 4371–4383 (2008).
3. E. H. Warren, H. J. Deeg, Dissecting graft-versus-leukemia from graft-versus-host-disease using novel strategies. *Tissue Antigens* **81**, 183–193 (2013).
4. W. D. Shlomchik, Graft-versus-host disease. *Nat. Rev. Immunol.* **7**, 340–352 (2007).
5. K. A. Markey, K. P. MacDonald, G. R. Hill, The biology of graft-versus-host disease: Experimental systems instructing clinical practice. *Blood* **124**, 354–362 (2014).
6. N. J. Chao, B. J. Chen, Prophylaxis and treatment of acute graft-versus-host disease. *Semin. Hematol.* **43**, 32–41 (2006).
7. S. G. Holtan, M. Pasquini, D. J. Weisdorf, Acute graft-versus-host disease: A bench-to-bedside update. *Blood* **124**, 363–373 (2014).
8. S. W. Choi, P. Reddy, Current and emerging strategies for the prevention of graft-versus-host disease. *Nat. Rev. Clin. Oncol.* **11**, 536–547 (2014).
9. V. T. Ho, R. J. Soiffer, The history and future of T-cell depletion as graft-versus-host disease prophylaxis for allogeneic hematopoietic stem cell transplantation. *Blood* **98**, 3192–3204 (2001).
10. M. T. Vander Lugt, T. M. Braun, S. Hanash, J. Ritz, V. T. Ho, J. H. Antin, Q. Zhang, C.-H. Wong, H. Wang, A. Chin, A. Gomez, A. C. Harris, J. E. Levine, S. W. Choi, D. Couriel, P. Reddy, J. L. Ferrara, S. Paczesny, ST2 as a marker for risk of therapy-resistant graft-versus-host disease and death. *N. Engl. J. Med.* **369**, 529–539 (2013).
11. C. Garlanda, C. A. Dinarello, A. Mantovani, The interleukin-1 family: Back to the future. *Immunity* **39**, 1003–1018 (2013).
12. H. Iwahana, K. Yanagisawa, A. Ito-Kosaka, K. Kuroiwa, K. Tago, N. Komatsu, R. Katashima, M. Itakura, S. Tominaga, Different promoter usage and multiple transcription initiation sites of the interleukin-1 receptor-related human ST2 gene in UT-7 and TM12 cells. *Eur. J. Biochem.* **264**, 397–406 (1999).
13. J. Schmitz, A. Owyang, E. Oldham, Y. Song, E. Murphy, T. K. McClanahan, G. Zurawski, M. Moshrefi, J. Qin, X. Li, D. M. Gorman, J. F. Bazan, R. A. Kastelein, IL-33, an interleukin-1-like cytokine that signals via the IL-1 receptor-related protein ST2 and induces T helper type 2-associated cytokines. *Immunity* **23**, 479–490 (2005).
14. K. Yanagisawa, Y. Naito, K. Kuroiwa, T. Arai, Y. Furukawa, H. Tomizuka, Y. Miura, T. Kasahara, T. Tetsuka, S. Tominaga, The expression of ST2 gene in helper T cells and the binding of ST2 protein to myeloma-derived RPMI8226 cells. *J. Biochem.* **121**, 95–103 (1997).
15. M. Löhning, A. Stroehmann, A. J. Coyle, J. L. Grogan, S. Lin, J.-C. Gutierrez-Ramos, D. Levinson, A. Radbruch, T. Kamradt, T1/ST2 is preferentially expressed on murine Th2 cells, independent of interleukin 4, interleukin 5, and interleukin 10, and important for Th2 effector function. *Proc. Natl. Acad. Sci. U.S.A.* **95**, 6930–6935 (1998).
16. D. Xu, W. Chan, B. P. Leung, F. Huang, R. Wheeler, D. Piedrafita, J. H. Robinson, F. Y. Liew, Selective expression of a stable cell surface molecule on type 2 but not type 1 helper T cells. *J. Exp. Med.* **187**, 787–794 (1998).
17. K. Oshikawa, K. Yanagisawa, S. Tominaga, Y. Sugiyama, Expression and function of the ST2 gene in a murine model of allergic airway inflammation. *Clin. Exp. Allergy* **32**, 1520–1526 (2002).
18. H. Hayakawa, M. Hayakawa, A. Kume, S. Tominaga, Soluble ST2 blocks interleukin-33 signaling in allergic airway inflammation. *J. Biol. Chem.* **282**, 26369–26380 (2007).
19. S. Sanada, D. Hakuno, L. J. Higgins, E. R. Schreiter, A. N. McKenzie, R. T. Lee, IL-33 and ST2 comprise a critical biomechanically induced and cardioprotective signaling system. *J. Clin. Invest.* **117**, 1538–1549 (2007).
20. D. A. Pascual-Figal, I. P. Garrido, R. Blanco, A. Minguela, A. Lax, J. Ordoñez-Llanos, A. Bayes-Genis, M. Valdés, S. A. Moore, J. L. Januzzi, Soluble ST2 is a marker for acute cardiac allograft rejection. *Ann. Thorac. Surg.* **92**, 2118–2124 (2011).
21. H. R. Turnquist, Z. Zhao, B. R. Rosborough, Q. Liu, A. Castellaneta, K. Isse, Z. Wang, M. Lang, D. B. Stolz, X. X. Zheng, A. J. Demetris, F. Y. Liew, K. J. Wood, A. W. Thomson, IL-33 expands suppressive CD11b$^+$ Gr-1^{int} and regulatory T cells, including ST2L$^+$ Foxp3$^+$ cells, and mediates regulatory T cell-dependent promotion of cardiac allograft survival. *J. Immunol.* **187**, 4598–4610 (2011).
22. S. M. Brunner, G. Schiechl, W. Falk, H. J. Schlitt, E. K. Geissler, S. Fichtner-Feigl, Interleukin-33 prolongs allograft survival during chronic cardiac rejection. *Transpl. Int.* **24**, 1027–1039 (2011).
23. L. Pastorelli, R. R. Garg, S. B. Hoang, L. Spina, B. Mattioli, M. Scarpa, C. Fiocchi, M. Vecchi, T. T. Pizarro, Epithelial-derived IL-33 and its receptor ST2 are dysregulated in ulcerative colitis and in experimental Th1/Th2 driven enteritis. *Proc. Natl. Acad. Sci. U.S.A.* **107**, 8017–8022 (2010).
24. D. Diaz-Jiménez, L. E. Nuñez, C. J. Beltrán, E. Candia, C. Suazo, M. Álvarez-Lobos, M.-J. González, M. A. Hermoso, R. Quera, Soluble ST2: A new and promising activity marker in ulcerative colitis. *World J. Gastroenterol.* **17**, 2181–2190 (2011).
25. C. Schiering, T. Krausgruber, A. Chomka, A. Fröhlich, K. Adelmann, E. A. Wohlfert, J. Pott, T. Griseri, J. Bollrath, A. N. Hegazy, O. J. Harrison, B. M. Owens, M. Löhning, Y. Belkaid, P. G. Fallon, F. Powrie, The alarmin IL-33 promotes regulatory T-cell function in the intestine. *Nature* **513**, 564–568 (2014).
26. N. Fursov, E. Johnston, K. Duffy, A. Cotty, T. Petley, J. Fisher, H. Jiang, M. A. Rycyzyn, J. Giles-Komar, G. Powers, Generation and characterization of rat anti-mouse ST2L monoclonal antibodies. *Hybridoma (Larchmt)* **30**, 153–162 (2011).
27. S. Manzano-Fernández, T. Mueller, D. Pascual-Figal, Q. A. Truong, J. L. Januzzi, Usefulness of soluble concentrations of interleukin family member ST2 as predictor of mortality in patients with acutely decompensated heart failure relative to left ventricular ejection fraction. *Am. J. Cardiol.* **107**, 259–267 (2011).
28. B. Johansson-Lindbom, M. Svensson, O. Pabst, C. Palmqvist, G. Marquez, R. Forster, W. W. Agace, Functional specialization of gut CD103$^+$ dendritic cells in the regulation of tissue-selective T cell homing. *J. Exp. Med.* **202**, 1063–1073 (2005).
29. J.-X. Wang, S. Kaieda, S. Ameri, N. Fishgal, D. Dwyer, A. Dellinger, C. L. Kepley, M. F. Gurish, P. A. Nigrovic, IL-33/ST2 axis promotes mast cell survival via BCLXL. *Proc. Natl. Acad. Sci. U.S.A.* **111**, 10281–10286 (2014).
30. D. B. Leveson-Gower, E. I. Sega, J. Kalesnikoff, M. Florek, Y. Pan, A. Pierini, S. J. Galli, R. S. Negrin, Mast cells suppress murine GVHD in a mechanism independent of CD4$^+$CD25$^+$ regulatory T cells. *Blood* **122**, 3659–3665 (2013).
31. C. Cocco, E. Di Carlo, S. Zupo, S. Canale, A. Zorzoli, D. Ribatti, F. Morandi, E. Ognio, I. Airoldi, Complementary IL-23 and IL-27 anti-tumor activities cause strong inhibition of human follicular and diffuse large B-cell lymphoma growth in vivo. *Leukemia* **26**, 1365–1374 (2012).
32. M. Hisada, S. Kamiya, K. Fujita, M. L. Belladonna, T. Aoki, Y. Koyanagi, J. Mizuguchi, T. Yoshimoto, Potent antitumor activity of interleukin-27. *Cancer Res.* **64**, 1152–1156 (2004).
33. W. Hashimoto, T. Osaki, H. Okamura, P. D. Robbins, M. Kurimoto, S. Nagata, M. T. Lotze, H. Tahara, Differential antitumor effects of administration of recombinant IL-18 or recombinant IL-12 are

mediated primarily by Fas-Fas ligand- and perforin-induced tumor apoptosis, respectively. *J. Immunol.* **163**, 583–589 (1999).
34. Y. Lu, S. Hong, H. Li, J. Park, B. Hong, L. Wang, Y. Zheng, Z. Liu, J. Xu, J. He, J. Yang, J. Qian, Q. Yi, Th9 cells promote antitumor immune responses in vivo. *J. Clin. Invest.* **122**, 4160–4171 (2012).
35. Y. Lu, B. Hong, H. Li, Y. Zheng, M. Zhang, S. Wang, J. Qian, Q. Yi, Tumor-specific IL-9–producing $CD8^+$ Tc9 cells are superior effector than type-I cytotoxic Tc1 cells for adoptive immunotherapy of cancers. *Proc. Natl. Acad. Sci. U.S.A.* **111**, 2265–2270 (2014).
36. R. J. Robb, E. Kreijveld, R. D. Kuns, Y. A. Wilson, S. D. Olver, A. L. Don, N. C. Raffelt, N. A. De Weerd, K. E. Lineburg, A. Varelias, K. A. Markey, M. Koyama, A. D. Clouston, P. J. Hertzog, K. P. Macdonald, G. R. Hill, Type I-IFNs control GVHD and GVL responses after transplantation. *Blood* **118**, 3399–3409 (2011).
37. S. P. Cullen, M. Brunet, S. J. Martin, Granzymes in cancer and immunity. *Cell Death Differ.* **17**, 616–623 (2010).
38. T. C. P. Somervaille, M. L. Cleary, Identification and characterization of leukemia stem cells in murine MLL-AF9 acute myeloid leukemia. *Cancer Cell* **10**, 257–268 (2006).
39. A. V. Krivtsov, D. Twomey, Z. Feng, M. C. Stubbs, Y. Wang, J. Faber, J. E. Levine, J. Wang, W. C. Hahn, D. G. Gilliland, T. R. Golub, S. A. Armstrong, Transformation from committed progenitor to leukaemia stem cell initiated by MLL-AF9. *Nature* **442**, 818–822 (2006).
40. L. C. Sjöberg, J. A. Gregory, S.-E. Dahlén, G. P. Nilsson, M. Adner, Interleukin-33 exacerbates allergic bronchoconstriction in the mice via activation of mast cells. *Allergy* **70**, 514–521 (2015).
41. E. Bourgeois, L. P. Van, M. Samson, S. Diem, A. Barra, S. Roga, J.-M. Gombert, E. Schneider, M. Dy, P. Gourdy, J.-P. Girard, A. Herbelin, The pro-Th2 cytokine IL-33 directly interacts with invariant NKT and NK cells to induce IFN-γ production. *Eur. J. Immunol.* **39**, 1046–1055 (2009).
42. D. K. Reichenbach, V. Schwarze, B. M. Matta, V. Tkachev, E. Lieberknecht, Q. Liu, B. H. Koehn, D. Pfeifer, P. A. Taylor, G. Prinz, H. Dierbach, N. Stickel, Y. Beck, M. Warncke, T. Junt, A. Schmitt-Graeff, S. Nakae, M. Follo, T. Wertheimer, L. Schwab, J. Devlin, S. C. Watkins, J. Duyster, J. L. Ferrara, H. R. Turnquist, R. Zeiser, B. R. Blazar, The IL-33/ST2 axis augments effector T-cell responses during acute GVHD. *Blood* **125**, 3183–3192 (2015).
43. S. Lécart, N. Lecointe, A. Subramaniam, S. Alkan, D. Ni, R. Chen, V. Boulay, J. Pène, K. Kuroiwa, S. Tominaga, H. Yssel, Activated, but not resting human Th2 cells, in contrast to Th1 and T regulatory cells, produce soluble ST2 and express low levels of ST2L at the cell surface. *Eur. J. Immunol.* **32**, 2979–2987 (2002).
44. E. Zorn, H. T. Kim, S. J. Lee, B. H. Floyd, D. Litsa, S. Arumugarajah, R. Bellucci, E. P. Alyea, J. H. Antin, R. J. Soiffer, J. Ritz, Reduced frequency of $FOXP3^+$ $CD4^+CD25^+$ regulatory T cells in patients with chronic graft-versus-host disease. *Blood* **106**, 2903–2911 (2005).
45. M. Edinger, P. Hoffmann, J. Ermann, K. Drago, C. G. Fathman, S. Strober, R. S. Negrin, $CD4^+CD25^+$ regulatory T cells preserve graft-versus-tumor activity while inhibiting graft-versus-host disease after bone marrow transplantation. *Nat. Med.* **9**, 1144–1150 (2003).
46. J. M. Magenau, X. Qin, I. Tawara, C. E. Rogers, C. Kitko, M. Schlough, D. Bickley, T. M. Braun, P.-S. Jang, K. P. Lowler, D. M. Jones, S. W. Choi, P. Reddy, S. Mineishi, J. E. Levine, J. L. Ferrara, S. Paczesny, Frequency of $CD4^+CD25^{hi}FOXP3^+$ regulatory T cells has diagnostic and prognostic value as a biomarker for acute graft-versus-host-disease. *Biol. Blood Marrow Transplant.* **16**, 907–914 (2010).
47. G. R. Hill, J. M. Crawford, K. R. Cooke, Y. S. Brinson, L. Pan, J. L. Ferrara, Total body irradiation and acute graft-versus-host disease: The role of gastrointestinal damage and inflammatory cytokines. *Blood* **90**, 3204–3213 (1997).
48. M. Koyama, R. D. Kuns, S. D. Olver, N. C. Raffelt, Y. A. Wilson, A. L. Don, K. E. Lineburg, M. Cheong, R. J. Robb, K. A. Markey, A. Varelias, B. Malissen, G. J. Hämmerling, A. D. Clouston, C. R. Engwerda, P. Bhat, K. P. MacDonald, G. R. Hill, Recipient nonhematopoietic antigen-presenting cells are sufficient to induce lethal acute graft-versus-host disease. *Nat. Med.* **18**, 135–142 (2012).
49. P. J. Martin, G. B. McDonald, J. E. Sanders, C. Anasetti, F. R. Appelbaum, H. J. Deeg, R. A. Nash, E. W. Petersdorf, J. A. Hansen, R. Storb, Increasingly frequent diagnosis of acute gastrointestinal graft-versus-host disease after allogeneic hematopoietic cell transplantation. *Biol. Blood Marrow Transplant.* **10**, 320–327 (2004).
50. M. L. MacMillan, D. J. Weisdorf, J. E. Wagner, T. E. DeFor, L. J. Burns, N. K. Ramsay, S. M. Davies, B. R. Blazar, Response of 443 patients to steroids as primary therapy for acute graft-versus-host disease: Comparison of grading systems. *Biol. Blood Marrow Transplant.* **8**, 387–394 (2002).
51. K. Hong, Y. Lee, S. Lee, S. Hong, S. Bae, J. Hong, J. Choi, H. Jhun, A. Kwak, E. Kim, S. Jo, T. Kang, Y. S. Cho, Y.-G. Kim, S. Kim, The inhibitory function of Fc-ST2 depends on cell type; IL-1RAcP and ST2 are necessary but insufficient for IL-33 activity. *Immunol. Res.* **56**, 122–130 (2013).
52. I. Tawara, M. Koyama, C. Liu, T. Toubai, D. Thomas, R. Evers, P. Chockley, E. Nieves, Y. Sun, K. P. Lowler, C. Malter, N. Nishimoto, G. R. Hill, P. Reddy, Interleukin-6 modulates graft-versus-host responses after experimental allogeneic bone marrow transplantation. *Clin. Cancer Res.* **17**, 77–88 (2011).
53. P. Reddy, Y. Sun, T. Toubai, R. Duran-Struuck, S. G. Clouthier, E. Weisiger, Y. Maeda, I. Tawara, O. Krijanovski, E. Gatza, C. Liu, C. Malter, P. Mascagni, C. A. Dinarello, J. L. Ferrara, Histone deacetylase inhibition modulates indoleamine 2,3-dioxygenase-dependent DC functions and regulates experimental graft-versus-host disease in mice. *J. Clin. Invest.* **118**, 2562–2573 (2008).
54. K. R. Cooke, L. Kobzik, T. R. Martin, J. Brewer, J. Delmonte Jr., J. M. Crawford, J. L. Ferrara, An experimental model of idiopathic pneumonia syndrome after bone marrow transplantation: I. The roles of minor H antigens and endotoxin. *Blood* **88**, 3230–3239 (1996).
55. G. R. Hill, K. R. Cooke, T. Teshima, J. M. Crawford, J. C. Keith Jr., Y. S. Brinson, D. Bungard, J. L. Ferrara, Interleukin-11 promotes T cell polarization and prevents acute graft-versus-host disease after allogeneic bone marrow transplantation. *J. Clin. Invest.* **102**, 115–123 (1998).
56. B. E. Anderson, P. A. Taylor, J. M. McNiff, D. Jain, A. J. Demetris, A. Panoskaltsis-Mortari, A. Ager, B. R. Blazar, W. D. Shlomchik, M. J. Shlomchik, Effects of donor T-cell trafficking and priming site on graft-versus-host disease induction by naive and memory phenotype CD4 T cells. *Blood* **111**, 5242–5251 (2008).
57. L. Lefrançois, N. Lycke, Isolation of mouse small intestinal intraepithelial lymphocytes, Peyer's patch, and lamina propria cells. *Curr. Protoc. Immunol.* **Chapter 3**, Unit 3.19 (2001).
58. A. S. Stephens, S. R. Stephens, N. A. Morrison, Internal control genes for quantitative RT-PCR expression analysis in mouse osteoblasts, osteoclasts and macrophages. *BMC Res. Notes* **4**, 410 (2011).
59. H. Hanenberg, X. L. Xiao, D. Dilloo, K. Hashino, I. Kato, D. A. Williams, Colocalization of retrovirus and target cells on specific fibronectin fragments increases genetic transduction of mammalian cells. *Nat. Med.* **2**, 876–882 (1996).

Acknowledgments: We thank the operators of the Indiana University Melvin and Bren Simon Cancer Center Flow Cytometry Resource Facility for their outstanding technical help. We also acknowledge the help and support of the In Vivo Therapeutics Core of the Indiana University Melvin and Bren Simon Cancer Center. We thank A. McKenzie from the Medical Research Council Laboratory of Molecular Biology, Cambridge, UK for providing the $ST2^{-/-}$ mice. We thank K. Duffy from Centocor, a pharmaceutical company of Johnson & Johnson, for providing the anti-ST2 mAb (CNT03914). We thank T. M. Braun of the University of Michigan for statistical services on sample size calculations for experimental GVHD models. We thank M. C. Pasquini and S. R. Spellman from the Center for International Blood and Marrow Transplant Research. **Funding:** This work was supported by the National Cancer Institute (R01CA168814 to S.P.), the Leukemia & Lymphoma Society Scholar Award (1293-15 to S.P.), the Lilly Physician Scientist Initiative Award (to S.P.), the Senshin Medical Research Foundation (to I.T.), and the National Institute of Allergy and Infectious Diseases (R01AI34495 to B.R.B.). The Flow Cytometry Resource Facility is partially funded by a National Cancer Institute grant (P30 CA082709). The In Vivo Therapeutics Core of the Indiana University Melvin and Bren Simon Cancer Center is partially funded by a National Cancer Institute grant (P30 CA082709) and a National Institute of Diabetes and Digestive and Kidney Diseases grant (P01 DK090948). **Author contributions:** J.Z. and A.M.R. designed and performed research, analyzed data, and wrote the paper; B.G. and W.L. performed research; M.J.T. contributed new mice and provided intellectual input; C.L. graded and scored GVHD histopathology; R.K. and H.H. provided essential materials and provided intellectual input; B.R.B. was involved in data discussions and manuscript editing; I.T. designed and performed research, analyzed data, and was involved in data discussions; S.P. conceived the project, designed experiments, analyzed data, and wrote the paper. **Competing interests:** S.P. has a patent on "Methods of detection of graft-versus-host disease" licensed to Viracor-IBT Laboratories. Otherwise, the authors declare that they have no competing interests.

Submitted 27 June 2015
Accepted 8 August 2015
Published 7 October 2015
10.1126/scitranslmed.aab0166

Citation: J. Zhang, A. M. Ramadan, B. Griesenauer, W. Li, M. J. Turner, C. Liu, R. Kapur, H. Hanenberg, B. R. Blazar, I. Tawara, S. Paczesny, ST2 blockade reduces sST2-producing T cells while maintaining protective mST2-expressing T cells during graft-versus-host disease. *Sci. Transl. Med.* **7**, 308ra160 (2015).

Science Translational Medicine

ST2 blockade reduces sST2-producing T cells while maintaining protective mST2-expressing T cells during graft-versus-host disease

Jilu Zhang, Abdulraouf M. Ramadan, Brad Griesenauer, Wei Li, Matthew J. Turner, Chen Liu, Reuben Kapur, Helmut Hanenberg, Bruce R. Blazar, Isao Tawara and Sophie Paczesny

Sci Transl Med **7**, 308ra160308ra160.
DOI: 10.1126/scitranslmed.aab0166

Blocking graft-versus-host disease

Bone marrow transplantation replaces unhealthy bone marrow with bone marrow from a healthy donor. However, the donor-derived immune cells may recognize the transplant recipient as foreign and attack, resulting in graft-versus-host disease (GVHD). Now, Zhang *et al.* report that blocking soluble suppression of tumorigenicity 2 (sST2), a plasma marker for GVHD, with a neutralizing antibody can reduce GVHD severity and mortality. The blockade decreased the production of proinflammatory cytokines and increased the frequency of anti-inflammatory molecules and cells while maintaining graft-versus-leukemia activity. These data suggest that targeting sST2 may help decrease GVHD after bone marrow transplantation.